

Magnetic interactions, weak ferromagnetism, and field-induced transitions in Nd_2NiO_4

X. Batlle*

Departament de Física Fonamental, Facultat de Física, Universitat de Barcelona, Diagonal 647, 08028 Barcelona, Spain

X. Obradors and B. Martínez

Institut de Ciència de Materials de Barcelona, Consejo Superior de Investigaciones Científicas, Campus Universitari de Bellaterra, 08193 Cerdanyola (Barcelona), Spain

(Received 28 March 1991)

The magnetic properties of stoichiometric Nd_2NiO_4 have been investigated by means of dc- and ac-magnetic-susceptibility and isothermal-magnetization measurements. Five different magnetic phase transitions have been identified and characterized. A collinear antiferromagnetic ordering of Ni^{2+} magnetic moments exists between $T_{N1} \approx 320$ K and $T_{C1} \approx 130$ K (g_x mode) where an orthorhombic-to-tetragonal ($Bmab$ to $P4_2/nm$) structural phase transition occurs. In this temperature range, the Nd^{3+} ions behave as a paramagnet being polarized by the effect of an internal magnetic field associated with the Ni-Nd antiferromagnetic superexchange interaction. A weak ferromagnetic component appears below 130 K, which is consistent with the $g_x c_y f_z$ and $g_x + c_y f_z$ magnetic modes for Ni^{2+} proposed from a neutron-powder-diffraction experiment. An additional out-of-plane component of the internal magnetic field on the Nd^{3+} ions develops with this structural phase transition and strongly polarizes these ions. Two additional transitions are observed at $T_{c2} \approx 68$ K (very prominent) and $T_{c3} \approx 45$ K (very smooth), which are characterized by a sudden increase in the internal magnetic field acting on the Nd ions. This internal magnetic field is evaluated and an antiparallel ordering between the Ni and Nd weak ferromagnetic spin components is inferred. A field-induced transition has been identified. A peak on both the differential susceptibility and the real part of the ac susceptibility at $T_{N2} \approx 11$ K marks a long-range antiferromagnetic ordering of the Nd^{3+} ions. The out-of-plane component of the Ni^{2+} magnetic moments is attributed to the antisymmetric interaction $D_{\text{Ni-Ni}}$, which turns out to be quite important ($D_{\text{Ni-Ni}} \approx -16.0$ meV) as compared to La_2NiO_4 and La_2CuO_4 , probably because of a greater tilting angle of the octahedra. Finally, the magnetocrystalline anisotropy associated with Nd ions is found to be high below 20 K.

I. INTRODUCTION

The magnetic behavior of the nickelates of general formula $R_2\text{NiO}_4$ ($R = \text{La}, \text{Pr}, \text{Nd}$) has aroused considerable interest since the discovery of both p - and n -type high- T_c cuprate superconductors¹ mainly because of the fact that the overall magnetic properties of nickelates and cuprates show strong similarities. However, no superconducting state has been clearly found in the nickelates, although some authors have claimed the occurrence of superconductivity in this system.²

From a magnetic point of view, the Cu and Ni sublattices behave in rather similar ways: in both cases a long-range three-dimensional (3D) antiferromagnetic order develops below about 320 K while strong 2D antiferromagnetic fluctuations persist above the Néel temperature.^{3,4} The magnetic behavior of the cuprates isomorphous to Nd_2CuO_4 appears much more complex because of R -Cu and R - R magnetic interactions which lead, in some cases, to a long-range magnetic ordering of the rare earths that may even coexist with the superconducting state.⁵ This interesting magnetic behavior is also observed in $(\text{Pr}, \text{Nd})_2\text{NiO}_4$ oxides.⁶⁻⁹ However, concerning the crystal structure, while $R_2\text{NiO}_4$ -type compounds remain iso-

morphous to La_2CuO_4 and both Ni and Cu exhibit an octahedral coordination, Nd_2CuO_4 -type compounds are tetragonal with a square-planar arrangement of the Cu-O atoms. Then, an understanding of the magnetic properties of La_2NiO_4 might clarify which facts are relevant in the occurrence of high- T_c superconductivity, while a parallel study on $(\text{Nd}, \text{Pr})_2\text{NiO}_4$ might shed some light on the role of the rare-earth-transition-metal (R -TM) magnetic interactions.

Referring to the crystallographic structure, $R_2\text{NiO}_4$ ($R = \text{La}, \text{Pr}, \text{Nd}$) oxides display some common signatures: above a certain temperature T_{c2} [La_2NiO_4 : $T_{c2} \approx 770$ K;^{10,11} Pr_2NiO_4 : $T_{c2} \approx 1520$ K;⁸ Nd_2NiO_4 : $T_{c2} \approx 1900$ K (Ref. 6)] the crystal structure is described in the $I4/mmm$ tetragonal space group, which is known as the T structure of the K_2NiF_4 -type compounds. Around this temperature, a second-order structural phase transition occurs and the crystal symmetry changes to orthorhombic ($Bmab$ space group). This transition is of the same kind as that observed in La_2CuO_4 at 530 K.¹² The orthorhombic distortion involves a slight rotation of the NiO_6 octahedra, in such a way that the tilting angle smoothly increases upon lowering temperature. Then, on reaching a critical value, the $Bmab$ structure is no longer stable and an orthorhombic-to-tetragonal ($Bmab$ to $P4_2/nm$)

first-order structural phase transition takes place at T_{c1} in order to rearrange the structure [La_2NiO_4 : $T_{c1} \approx 80$ K;^{10,11,13,14} Pr_2NiO_4 : $T_{c1} \approx 115$ K;^{8,9} Nd_2NiO_4 : $T_{c1} \approx 130$ K (Refs. 6 and 7)]. This low-temperature structural phase transition is similar to that observed in $\text{La}_{2-x}\text{Ba}_x\text{CuO}_4$,¹⁵ although it is not detected either in La_2CuO_4 or in $\text{La}_{2-x}\text{Sr}_x\text{CuO}_4$.

Likewise, in all three oxides, the Ni sublattice orders antiferromagnetically in the g_x magnetic mode as long as the crystallographic structure remains orthorhombic, and they have very similar Néel temperatures [La_2NiO_4 : $T_{N1} \approx 330$ K;^{4,10,11,14} Pr_2NiO_4 : $T_{N1} \approx 325$ K;⁸ Nd_2NiO_4 : $T_{N1} \approx 320$ K (Ref. 6), which appear to be very close to that of stoichiometric La_2CuO_4 ($T_{N1} \approx 320$ K).¹⁶ Below T_{c1} , the situation is more complex: the low-temperature tetragonal symmetry allows the existence of a weak ferromagnetic component along the c axis (out-of-plane axis). The magnetic structure may now be described either in the $g_x c_y f_z$ or $g_x + c_y f_z$ modes for both La_2NiO_4 and Nd_2NiO_4 , while in Pr_2NiO_4 there is a progressive spin reorientation from the $g_x c_y f_z$ mode to the $c_x g_y a_z$ mode as temperature falls, in such a way that at 1.5 K the latter represents the total of the magnetic order of Ni^{2+} ions. Finally, at some temperature below T_{c1} , Nd^{3+} and Pr^{3+} ions are strongly polarized, as evidenced by neutron powder diffraction,^{6,8} and this progressive ordering of the rare-earth sublattice occurs in the same magnetic mode as that of Ni. However, while Nd^{3+} ions present a long-range antiferromagnetic ordering at $T_{N2} \approx 11$ K, similarly to Nd_2CuO_4 ,¹⁷ the Pr^{3+} sublattice does not achieve any long-range ordering above 1.5 K. Furthermore, some other magnetic anomalies are detected in Nd_2NiO_4 and Pr_2NiO_4 at some intermediate temperatures, signaling the existence of spin reorientations probably related to those observed in Nd_2CuO_4 .¹⁸

Finally, it is worth stressing that neutron-powder-diffraction (NPD) results show^{6,8,10,11} that (i) in La_2NiO_4 , the magnetic moment for Ni is about $1.68\mu_B$ at 1.5 K (smaller than the spin-only value due to zero-point quantum fluctuations), while the ferromagnetic component along the c axis is too small to be detected; (ii) in Nd_2NiO_4 , the magnetic moments for Ni and Nd are, respectively, about $1.59\mu_B$ and $3.2\mu_B$ at 1.5 K (this last one in close agreement with the expected value from the $^4I_{9/2}$ ground state), and they subtend angles of 14.6° and 18.2° with the basal plane, respectively; (iii) in Pr_2NiO_4 , the magnetic moments for Ni and Pr are, respectively, about $1.56\mu_B$ and $1.28\mu_B$ at 1.5 K (this last one is much smaller than the expected value from the 3H_4 ground state due to the fact that this sublattice is only partially ordered), and they stand at angles of 19.3° and 42.2° with the basal plane, respectively.

In a previous study⁷ some of us reported preliminary macroscopic magnetization measurements on stoichiometric Nd_2NiO_4 identifying up to five different magnetic phase transitions, related either to cooperative long-range magnetic orderings (Ni and Nd ions) or to spin reorientations associated with the orthorhombic-tetragonal structural phase transition or with other unexplained mechanisms. We report here experimental data

that strongly support our first analysis, both in the ferromagnetic-like character of the magnetic properties of this oxide and in the evaluation of the internal magnetic field acting on the Nd ions below ($T < T_{c1}$) and above ($T > T_{c1}$) the weak ferromagnetic regime. We have identified a metamagnetic-like field-induced transition having a very different character from that observed in La_2CuO_4 ,^{19,20} which allows us to determine the superexchange isotropic coupling constant among the Ni and Nd sublattices. Finally, we discuss the appearance of the weak ferromagnetism in terms of the antisymmetric Ni-Ni superexchange interaction $D_{\text{Ni-Ni}}$ and the magneto-crystalline anisotropy associated with Nd ions.

II. EXPERIMENTAL

Stoichiometric Nd_2NiO_4 polycrystalline samples were obtained by the reduction of the oxidized precursor at 350°C under a dry hydrogen atmosphere and careful monitoring of the reduction process by thermogravimetry. The oxidized precursor sample was prepared by the ceramic method from stoichiometric amounts of Nd_2O_3 and NiO, which were intimately homogenized and fired at temperatures up to 1450°C in air and several intermediate grindings with an accumulated firing time of about 300 hours.^{7,11,21} This long annealing was performed in order to yield very good crystallinity. This is an important point in this system because after the low-temperature structural phase transition very severe strains appear in the crystallites and these seem to be enhanced by the preexisting defects. The yield of the chemical reaction was followed by both x-ray and neutron diffraction and no impurity was observed within the detection limit of these techniques. Neutron powder diffraction showed much narrower Bragg lines than those previously observed.⁶ No Ni^{3+} ions could be detected by iodometric titration.

Low-field dc and ac magnetic susceptibilities were measured by means of a Faraday balance (temperature range 14–300 K) and an ac susceptometer (temperature range 4–300 K), respectively. Isothermal magnetization measurements were performed both with a Quantum Design SQUID magnetometer (up to 5 T) and with the axial extraction technique (up to 20 T) of the Service National des Champs Intenses at Grenoble. These magnetic measurements showed that a tiny amount of metallic Ni existed in our sample, which was probably formed during the hydrogen reduction step. We evaluate the amount of metallic Ni in our sample to be smaller than 0.1% in weight.

III. RESULTS

A. ac and dc magnetic susceptibility

The temperature dependence of the low-field dc magnetic susceptibility was first studied in order to identify the different transitions observed in the neutron diffraction patterns. [Fig. 1(a)]. A clear susceptibility upturn becomes prominent at $T_{c1} = 130$ K. This temperature corresponds exactly to that at which the

orthorhombic-tetragonal phase transition occurs and thus implies that the change of the NiO_6 octahedra tilting axis associated with this structural phase transition also brings about a reorientation of the Ni magnetic moments. We will further discuss this first transition in the light of the magnetic field dependence of the magnetization and of the magnetic structure determined by neutron powder diffraction.

Above T_{c1} and up to room temperature, the dc magnetic susceptibility displays a typical Curie-Weiss behavior [Fig. 1(b)]. In this temperature range, the magnetic moments of the Ni^{2+} ions are ordered ($T_{N1}=320$ K) and their contribution to the magnetic susceptibility and basically temperature-independent, while the Nd^{3+} ions should behave like a paramagnet being polarized by the

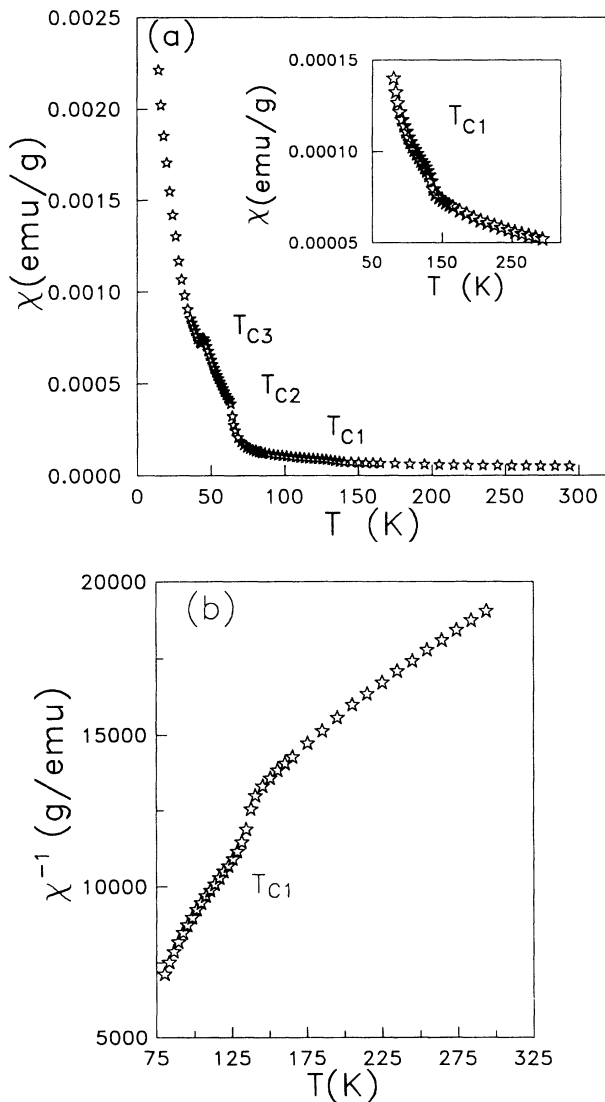


FIG. 1. (a) Low-field dc magnetic susceptibility ($H_{dc}=1.56$ kOe) of stoichiometric Nd_2NiO_4 in the temperature range 14–300 K. Inset: detail of the curve showing the structural phase transition at $T_{c1}=130$ K. (b) Inverse of the dc magnetic susceptibility ($H_{dc}=1.56$ kOe) in the temperature range 80–300 K.

effect of temperature.

Previous experimental data on Nd_2CuO_4 reported by Saez-Puche *et al.*²² and Seaman *et al.*,¹⁷ and more recently by Oseroff *et al.*,²³ show that no crystal-field effect is observed on Nd^{3+} ions above around 30 K and the magnetic moment derived from the inverse of the magnetic susceptibility corresponds exactly to that of Nd^{3+} ions [$\mu(\text{Nd}^{3+})=3.62\mu_B$, ground state $^4I_{9/2}$]. In this sense, we expected to find the same result in Nd_2NiO_4 . Nevertheless, when fitting the Curie-Weiss law to our experimental data, we obtain a magnetic moment which is roughly double. Later on, we will discuss this fact in the light of the internal magnetic field acting on Nd^{3+} ions as a result of the long-range magnetic ordering of the Ni sublattice.

On lowering temperature below T_{c1} , the dc magnetic susceptibility deviates from the linear law, signaling the appearance of the weak ferromagnetic component. As can be seen in Fig. 1(a), at about $T \approx 80$ K, a strong low-temperature polarization occurs which needs a thorough analysis. Two further transitions at $T_{c2} \approx 68$ K and $T_{c3} \approx 45$ K are observed in Fig. 1(a) which match the anomalies observed in the intensity of some magnetic Bragg reflections.⁶ These anomalies are superimposed on the strong low-temperature magnetic polarization of the Nd^{3+} ions.

The real part of the ac magnetic susceptibility χ' is represented in Fig. 2(a). Two prominent peaks and a smooth change of the curvature are well established; the first peak appears at $T_{N2} \approx 11$ K and may be related to the long-range order of the Nd ions. The second anomaly is found at $T_{c2} \approx 68$ K and it is more of an abrupt discontinuity rather than a peak. Finally, a smooth change of the curvature is seen around $T_{c3} \approx 45$ K, while no special effect is observed on crossing the orthorhombic-to-tetragonal structural phase transition at T_{c1} . All these findings have been clearly confirmed by both NPD and dc magnetic susceptibility. It is also worth pointing out that the inverse of the real part of the ac susceptibility also displays a Curie-Weiss behavior above T_{c1} , as indicated by the dc measurements [Fig. 2(a), inset].

The imaginary part of the ac magnetic susceptibility χ'' is displayed in Fig. 2(b), and it clearly shows a discontinuity at T_{c2} , signaling that some kind of first-order transition occurs at this temperature. In our opinion, this transition should have something to do with the competition between magnetocrystalline anisotropy and magnetic exchange: the faster temperature dependence of the former might account for a spin reorientation occurring on lowering the temperature below T_{c2} . Finally, a broad absorption peak is observed at low temperature around 25 K, while no special effect is detected at $T_{c3} \approx 45$ K. We believe that this latter transition might also be due to some kind of spin reorientation.

We have also studied the imaginary part of the ac susceptibility χ'' as a function of both frequency and intensity of the applied ac magnetic field. Concerning the absorption peak at 25 K, the out-of-phase component of the susceptibility indicates some kind of relaxation process.

For example, in paramagnets, the study of both χ' and χ'' as a function of frequency allows one to determine the time constants of the relaxation processes involved, thus leading to a standard way of dealing with this kind of phenomena.²⁴ In magnetically ordered systems, this technique is a direct method to analyze domain-wall relaxation with typical time constants of the order of 10^{-3} s, which dominates in the low-temperature regime.²⁵ In our case, the broad peak appearing at 25 K disappears for values of the external ac magnetic field lower than 0.1 Oe, which is consistent with the fact that the motion of a domain wall requires some minimum energy. The fact that the absorption peak is above $T_{N2} \approx 11$ K gives further confidence to the idea that it is basically related to a domain-wall relaxation process.

We have tried to determine the characteristic time constant for this process by measuring χ'' at different frequencies (from 10 Hz to 1000 Hz), but even at the maximum frequency accessible for our equipment (Lake-

Shore Susceptometer) we were not able to reach the maximum of the Argand diagram at 25 K. We were only able to assert that the relaxation time $\tau = 1/2\pi\nu^*$ is less than 10^{-4} s, where ν^* is the frequency at which the ratio χ''/χ' at a fixed temperature reaches its maximum. This value is smaller than the typical 10^{-3} s (Ref. 26) characteristic of the domain relaxation process, but it is still very far from other kinds of relaxation mechanisms, such as spin-spin (10^{-7} s) and spin-lattice (10^{-6} s) relaxation.

In order to explain this fact, we should bear in mind that we are dealing with a material of strong anisotropy, as we will point out when the magnetic field is inverted (see Fig. 4). This is a characteristic feature of ferromagnets with narrow domain walls that easily become pinned by structural defects. In this sense, the narrower the domain walls, the higher the energy associated with them, which leads to the decrease in the relaxation time, so we find smaller values of τ than those typically associated with domain wall relaxation mechanisms.

B. Isothermal magnetization curves $M(H)$

A much deeper insight into the microscopic mechanisms of the complex magnetic behavior of Nd_2NiO_4 may be gained from the isothermal magnetization curves.

In Fig. 3 we show some results, as a function of tem-

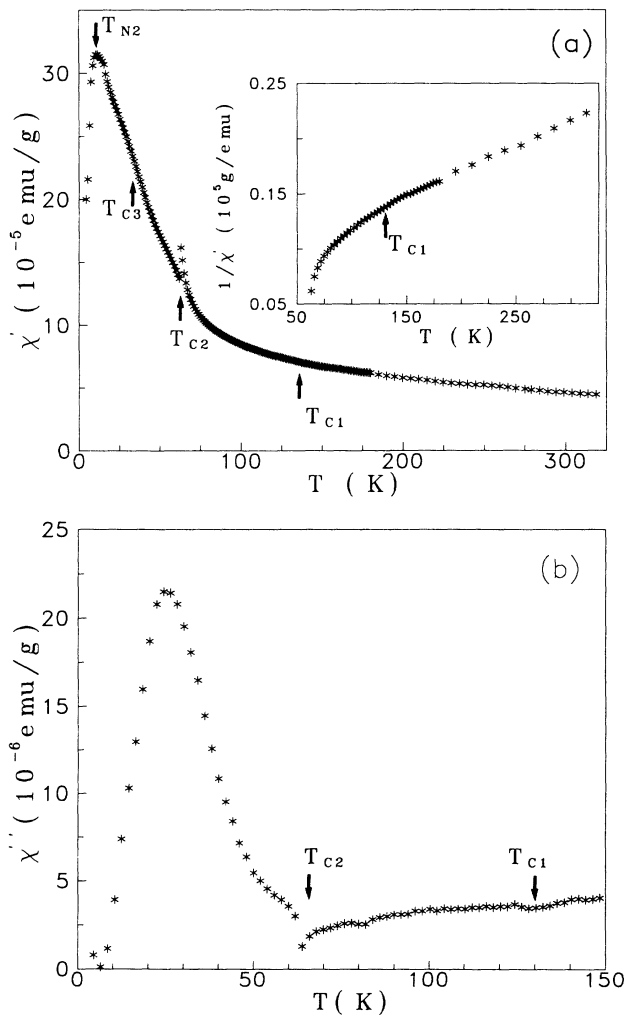


FIG. 2. (a) Real part of the ac magnetic susceptibility ($H_{ac} = 5$ Oe) at $\nu = 111.1$ Hz in the temperature range 4.2–300 K. Inset: inverse of the curve in the temperature range 80–300 K. (b) Imaginary part of the ac magnetic susceptibility ($H_{ac} = 5$ Oe) at $\nu = 111.1$ Hz in the temperature range 4.2–300 K.

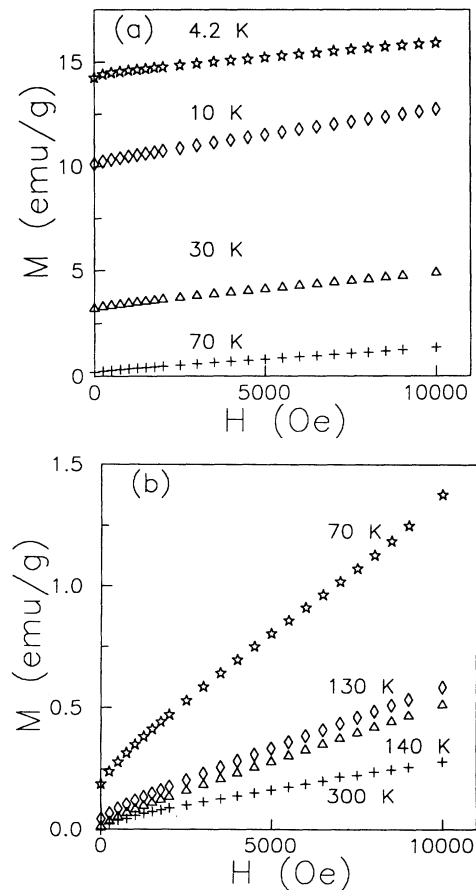


FIG. 3. Isothermal magnetization curves $M(H)$ (maximum applied field $H_{max} = 1$ T), as a function of temperature in the temperature range (a) 4.2–70 K and (b) 70–300 K.

perature, obtained on decreasing the magnetic field from $H = 1$ T, while in Fig. 4 a full hysteresis loop is displayed with a maximum magnetic field of $H = 5$ T. From these curves, the typical ferromagneticlike appearance of the magnetic properties of this oxide is very clear.

It should first be noted that the observed magnetization values are strongly dependent on the maximum previously applied field. This is an indication of ferromagnetic domains which cannot be completely reversed even with the application of magnetic fields up to 5 T, thus implying that the magnetic anisotropy of Nd_2NiO_4 should be high. This is further corroborated by the observation of anomalous drops in the hysteresis loop when the magnetic field is inverted (Fig. 4), which is also a typical feature of ferromagnets with narrow domain walls (strong anisotropy) which easily become pinned by structural defects.

The unusually high coercive field observed is also remarkable ($H_c = 1.1$ T at $T = 4.2$ K), which is consistent with a large magnetic anisotropy at low temperature. This is clearly singular as compared to $(\text{La}, \text{Nd}, \text{Gd})_2\text{CuO}_4$ and La_2NiO_4 oxides which have either null or very small coercive fields.^{13, 19, 20, 27} Furthermore, the coercive field of Nd_2NiO_4 is highly temperature dependent (for instance, $H_c = 1200$ Oe at $T = 70$ K), thus signaling that the magnetic anisotropy rapidly decreases with temperature, and becomes practically zero when $T > T_{c1}$, which reinforces the idea of the development of the ferromagnetic component below this temperature (Fig. 5).

It should also be mentioned that these isothermal magnetization curves do not display, up to maximum applied field of 5 T, any magnetically induced phase transition, in contrast to La_2CuO_4 .^{19, 20} In the latter, this field-induced transition was caused by a metamagneticlike transition of the weak ferromagnetic component which orders antiferromagnetically ($g_y a_z$ representation). The nonobservance of this sudden transition in Nd_2NiO_4 , but a progressive domain-wall inversion of the ferromagnetic components,

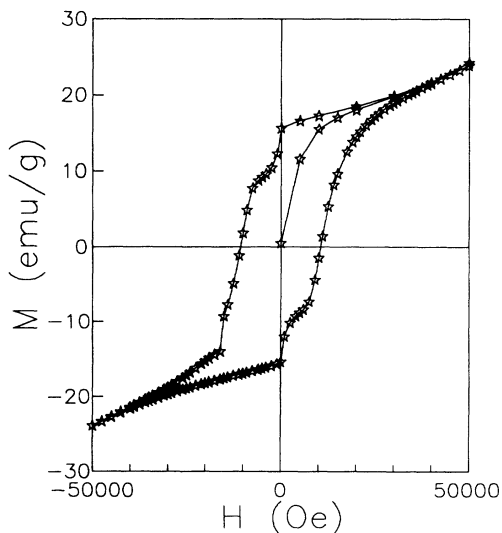


FIG. 4. Hysteresis curve at 4.2 K ($H_{\text{max}} = 5$ T).

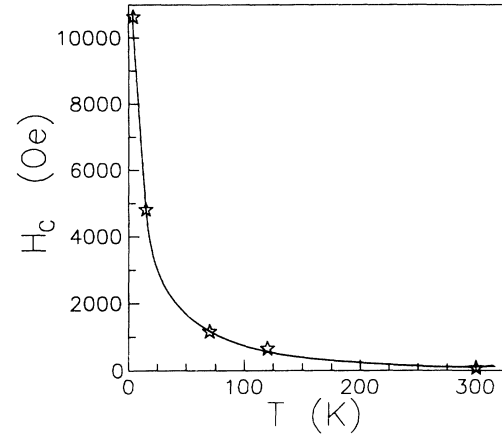


FIG. 5. Coercive field H_c as a function of temperature ($H_{\text{max}} = 5$ T).

is consistent with the magnetic representations obtained by the neutron diffraction study of Nd_2NiO_4 (Ref. 6) ($g_x c_y f_z$ or $g_x + c_y f_z$ representations below $T_{c1} = 130$ K). These magnetic modes indicate the existence of a ferromagnetic component along the c axis, instead of the antiferromagnetic one observed in La_2CuO_4 .

In Fig. 6, we represent the $M(H)$ curve at $T = 4.2$ K, measured on decreasing the magnetic field from $H_{\text{max}} = 20$ T. In Fig. 7 we display the magnetization values at different fields ($H = 0, 1,$ and 5 T), as a function of the maximum previously applied magnetic field (up to 20 T). These new data are of the greatest importance in order to clarify our basic experimental framework: Fig. 6 clearly shows that some kind of field-induced transition occurs. This transition is smooth (it takes place in the field range 3.5–6 T), since our sample is polycrystalline.

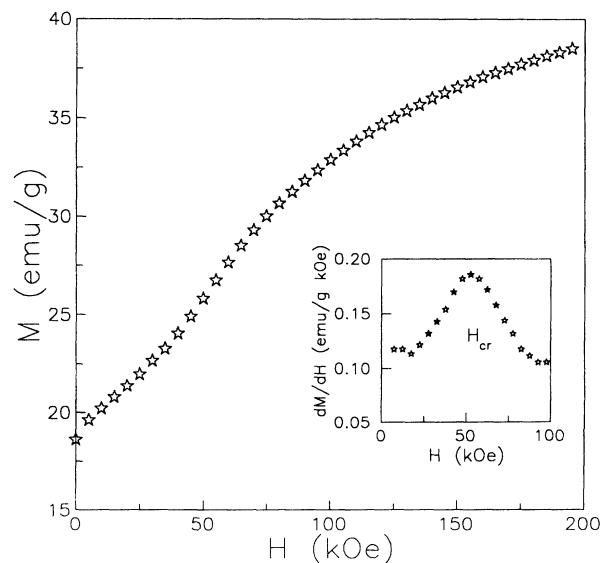


FIG. 6. (a) Isothermal magnetization curves at 4.2 K, with a maximum applied field of $H_{\text{max}} = 20$ T. Inset: derivative of the magnetization with respect to the applied field, as a function of the magnetic field, showing the critical field $H_{\text{cr}} = 5.2(2)$ T.

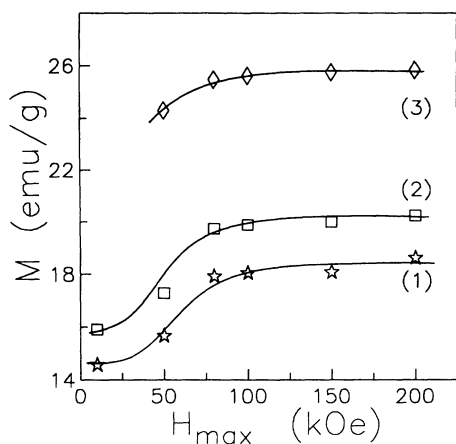


FIG. 7. Magnetization as a function of the maximum applied field ($T=4.2$ K), for different magnetic fields: (1) $H=0$ (remanence), (2) $H=1$ T, and (3) $H=5$ T.

Figure 7 evidences that the magnetic domains only disappear above $H \approx 8$ T.

We have evaluated the critical field H_{cr} at which the jump occurs from the inflection point of the curve (inset of Fig. 6) and we find that $H_{cr}=5.2(2)$ T at $T=4.2$ K, which is neither dependent on the maximum previously applied field nor very far from that reported in La_2CuO_4 (Ref. 26) [$H_{cr}=5.3(3)$ T when $T=0$]. The value of H_{cr} derived in this way indicates that the effects of the domain wall inversion are also superimposed in the field region where the magnetization jump takes place.

Then, this full analysis of the experimental characteristics of the $M(H)$ curves reveals that in stoichiometric Nd_2NiO_4 a magnetic domain structure (which is not present in La_2CuO_4) coexists with a metamagneticlike field-induced transition. Later on in this work we will explain the reasons for the occurrence of these effects at the same time.

When looking to the overall character of the $M(H)$ curves (Fig. 3) below the critical field, it is easy to conclude that they may be represented in a wide temperature range by the equation

$$M(H, T) = M_0(T) + \chi_d H_a, \quad (1)$$

where χ_d is a high-field differential susceptibility, H_a is the applied magnetic field, and $M_0(T)$ is the magnetization extrapolated at zero magnetic field from the linear high-field regime. This $M_0(T)$ is strongly temperature dependent and it is very near to the remanence because of the nearly linear character of the isothermal magnetization curves. The temperature dependence of the differential susceptibility χ_d and the zero-field extrapolated magnetization $M_0(T)$ are displayed in Figs. 8 and 9, respectively.

We note first that the ferromagnetic component develops at $T_{c1}=130$ K (both M_0 and χ_d exhibit a jump at this temperature), i.e., at the structural phase transition. The first-order character of this phase transition may be evidenced by the existence of some magnetization hysteresis

when cycling the temperature. Only a very small magnetic hysteresis remained above T_{c1} , which we attribute to a tiny amount of metallic Ni formed during the high-temperature hydrogen reduction step. The residual saturation magnetization of 0.05 emu/g at 300 K that we have found in the magnetization measurements lead us to evaluate the amount of metallic Ni in our sample to be smaller than 0.1% in weight. In any case, there is no doubt about the increase of the weak ferromagnetic component at T_{c1} , thus giving full support to the group-theoretical arguments which show that no weak ferromagnetic component is possible within the space group $Bmab$ in connection with the g mode.⁶

We should also take into account that this weak ferromagnetic component of the Ni magnetic moments lies at the origin of the magnetic anomaly observed in stoichiometric La_2NiO_4 ,¹³ where the structural phase

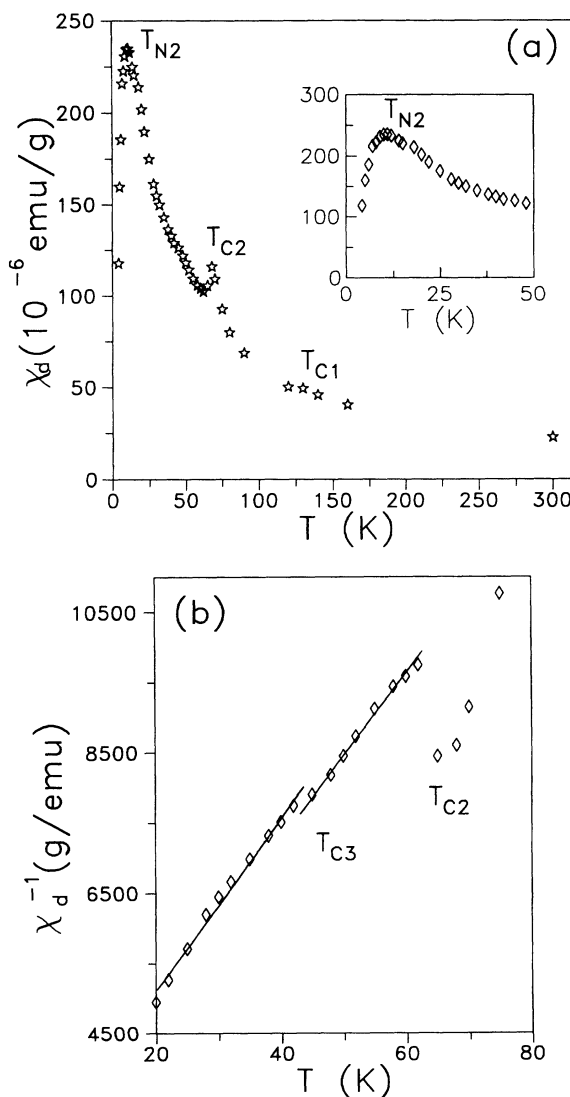


FIG. 8. (a) High-field differential susceptibility χ_d as a function of temperature. Inset: detail of the curve in the temperature range 4.2–50 K. (b) Detail of the inverse of the high-field differential susceptibility in the temperature range 20–80 K.

transition occurs at 80 K. This is also the temperature at which it was claimed that minor phase high-temperature superconductivity develops in La_2NiO_4 ,² and so we would like to stress that extreme care should be taken when observing magnetic anomalies around this temperature.

The existence of further spin reorientations at $T_{c2} \approx 68$ K and $T_{c3} \approx 45$ K may be clearly stated from the anomalies observed in either the high-field magnetic susceptibility or the saturation magnetization (Figs. 1,2,8,9). The observation of these anomalies in the region where the Nd ions are becoming progressively polarized by an internal magnetic field points to the existence of sudden increases in the c -axis component of this field.

It is not possible from our present macroscopic measurements on polycrystalline samples to undertake a complete analysis of these spin-reorientation transitions. It is very likely, however, that these anomalies involve some kind of spin reorientations, similar to those observed in Nd_2CuO_4 ,¹⁸ and there is probably competition between magnetocrystalline anisotropy and magnetic exchange effects.

Finally, a sharp peak at $T_{N2} \approx 11$ K is clearly observed in the the $\chi_d(T)$ curve [Fig. 8(a)], which is also evidenced

by the ac magnetic susceptibility [Fig. 2(a)], signaling a long-range magnetic ordering of the Nd ions. It is straightforward to note that this transition is hardly seen in the $M_0(T)$ curve, thus implying that the c -axis component of the internal magnetic field acting on the Nd ions is not modified by the long-range order of these ions. This observation is in sharp contrast with the behavior of T cuprates such as Gd_2CuO_4 ,²⁷ where the internal magnetic field falls to zero when the Gd ions order magnetically. It is also important to note that the long-range order transition identified here occurs at much higher temperatures than those observed in Nd_2CuO_4 ($T_N = 1.5$ K),¹⁷ even if in both cases a strong polarization of Nd ions magnetic moments is induced by the Ni or Cu sublattice.^{6,18}

IV. DISCUSSION

A. $T_{N1} > T > T_{c1}$

In this temperature range, the crystal symmetry ($Bmab$ orthorhombic space group) in connection with the g -mode does not allow the existence of a ferromagnetic component of the Ni^{2+} magnetic moments along the c axis; thus they are restricted to the a - b plane. Then, the in-plane ordered Ni^{2+} magnetic moments will cause a net in-plane staggered exchange internal field H_i^{a-b} acting on the Nd ions. Nevertheless, since H_i^{a-b} is antiferromagnetically staggered (due to the AF ordering of the Ni sublattice) no net magnetization in the Nd sublattice should be observed and Nd ions should follow a paramagnetic-like behavior, which is proved by the Curie-Weiss-like law evidenced by both dc and ac magnetic susceptibility above T_{c1} .

However, the external applied field H_a will induce a net magnetization of Ni^{2+} ions (which is not staggered but aligned along the magnetic field axis), which, at the same time, will polarize Nd^{3+} ions through an internal magnetic field H_i . What makes this argument appealing is the fact that the Nd ions are now being polarized by the effect both of the external applied field H_a and the internal induced magnetic field H_i . This means that the magnetic susceptibility may be expressed (assuming that above T_{c1} no crystal-field effects are expected on Nd^{3+} ions) as

$$\chi = C^*/T - \theta + \chi_0, \quad (2)$$

where χ_0 accounts for the temperature-independent contributions to the susceptibility, such as, for example, the core diamagnetism and the contribution arising from the antiferromagnetically ordered Ni sublattice [we assume this latter because the magnetic susceptibility of stoichiometric La_2NiO_2 is basically temperature-independent above 150 K (Ref. 13)].

As we can see, the effective Curie constant $C^* = C_{\text{Nd}}(1 + H_i/H_a)$ is greater than the expected C_{Nd} ($= 1.64$ emu K/mol) by a factor H_i/H_a .²⁸ For example, we have found experimentally by means of dc susceptibility [Fig. 1(b)] that $C^* = 6.0(2)$ emu K/mol when $H_a = 1.56$ kOe (which is of course much greater than the

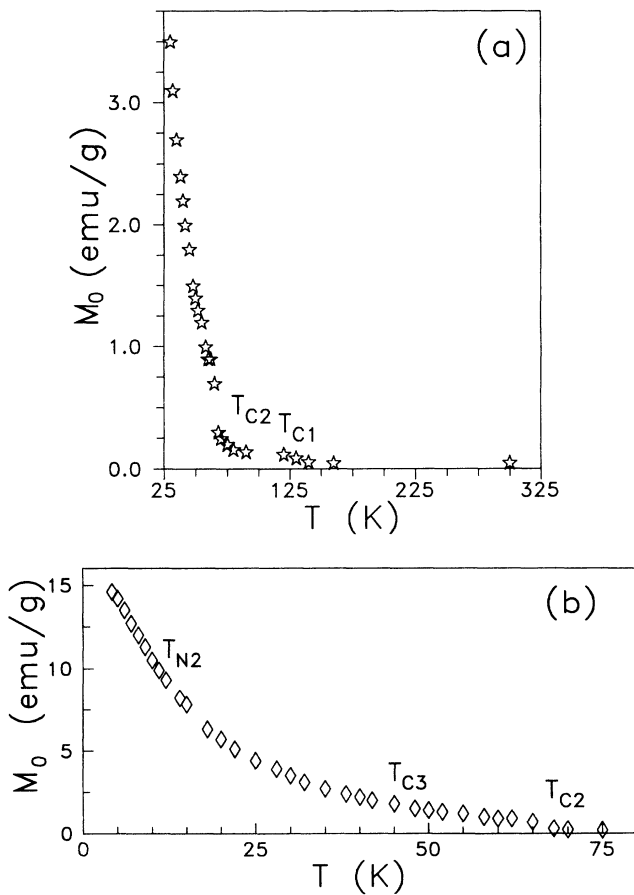


FIG. 9. Saturation magnetization M_0 as a function of temperature, in the temperature range (a) 25–300 K and (b) 4.2–75 K.

expected value for Nd^{3+} ions). This means that the induced internal magnetic field acting on Nd ions is about $H_i \approx 4.1(3)$ kOe.

Further support to our argument can be achieved as follows: in the scope of the mean-field approximation and assuming the Nd-Ni superexchange $J_{\text{Nd-Ni}}$ interaction to be isotropic, the induced internal magnetic field H_i acting on Nd ions and arising from the field induced magnetization of Ni ions may be written

$$H_i = (2ZJ_{\text{Nd-Ni}}/Ng_{\text{Nd}}g_{\text{Nd}}\mu_B^2)M_{\text{Ni}}, \quad (3)$$

where Z is the number of nearest neighbors, $g_{\text{Nd}} = \frac{8}{11}$, and M_{Ni} stands for the Ni sublattice magnetization. Expressing $M_{\text{Ni}} = \chi_{\text{Ni}}H_a$, Eq. (3) becomes

$$H_i = AM_{\text{Ni}} = A\chi_{\text{Ni}}H_a, \quad (4)$$

where A represents the molecular field constant characteristic of the mean-field approximation, thus suggesting that the effective Curie constant C^* should be temperature independent [$C^* = C_{\text{Nd}}(1 + A\chi_{\text{Ni}})$]. From our experimental data [$H_i \approx 4.1(3)$ kOe and $H_a = 1.56$ kOe], and assuming that the Ni sublattice magnetic susceptibility χ_{Ni} should be of the same order of magnitude as the value we have obtained for stoichiometric La_2NiO_4 (Ref. 13) [$\chi(300 \text{ K}) \approx 1.6 \times 10^{-6}$ emu/g, $\chi(150 \text{ K}) \approx 1.5 \times 10^{-6}$ emu/g], we derive that $J_{\text{Nd-Ni}} \approx 0.75(1)$ meV, which is in close agreement with the value we determine in the next section of this paper, where we derive that the Nd and Ni magnetic moments are antiparallel and $J_{\text{Nd-Ni}} = 0.6(2)$ meV.

B. $T_{c1} > T > T_{N2}$

Below T_{c1} , the new crystal symmetry ($P4_2/ncm$ tetragonal space group) allows the appearance of a weak ferromagnetic component of Ni^{2+} magnetic moments along the c axis, which develops an out-of-plane component of the internal field that further polarizes the Nd^{3+} ions and this is on the basis of the strong contribution of these ions to the magnetic susceptibility, mainly below 80 K [Figs. 1(a) and 2(a)]. The total internal field acting on Nd ions will basically be a consequence of the Nd-Ni exchange interaction and may be expressed as

$$H_i = H_i^0 + A\chi_{\text{Nd}}H_a, \quad (5)$$

where $A\chi_{\text{Nd}}H_a$ stands for the internal magnetic field arising from the field-induced magnetization of Ni ions [see Eq. (4)]. This contribution tends to zero with the applied field, while the term H_i^0 accounts for the internal field induced by the weak ferromagnetic component of the Ni^{2+} magnetic moments, which is not field dependent.

Then, if we assume the Nd-Ni superexchange coupling to be isotropic, H_i^0 may be written, in the scope of the mean-field approximation,

$$H_i^0 = 2ZJ_{\text{Nd-Ni}}\langle S_{\text{Ni}} \rangle^Z/g_{\text{Nd}}\mu_B, \quad (6)$$

thus meaning that the weak ferromagnetic component of

the Ni^{2+} magnetic moments ($\langle S_{\text{Ni}} \rangle^Z \neq 0$) originates an out-of-plane component of the internal magnetic field H_i^0 . Then, we assume that the c component of the internal field is on the origin of the strong polarization of Nd^{3+} , giving way to the strong increase in the saturation magnetization M_0 mainly below 80 K (Fig. 9). It is evident that this increase of the ferromagnetic component could also be related to the magnetic anisotropy, though in the next section we show that this latter contribution is not relevant above 20 K.

Let us now undertake the evaluation of the internal field acting on Nd ions and the origin of the field-induced transition:

1. Evaluation of internal field acting on Nd ions

Within the weak ferromagnetic regime ($T < T_{c1}$), a nonmonotonic magnetic behavior is observed with three more transitions at $T_{c2} \approx 68$ K, $T_{c3} \approx 45$ K and $T_{N2} \approx 11$ K (Figs. 1, 2, 8, and 9). If we concentrate on the $T_{c1} > T > T_{N2}$ temperature range, we may associate the two intermediate transitions (T_{c2} and T_{c3}) to some kind of spins reorientations coming from competition among magnetocrystalline anisotropy and magnetic exchange, leading to an increase in the saturation magnetization (Fig. 9).

If we now examine the magnetic behavior below T_{c2} , we see that the high-field magnetic susceptibility χ_d follows a Curie-Weiss law in two definite temperatures ranges; from T_{c2} to T_{c3} and from T_{c3} down to $T \approx 20$ K [Fig. 8(b)]. This fact suggest that, although the internal magnetic field acting on the Nd ions remains constant in each temperature interval, there exists some discontinuity on crossing T_{c3} .

On the other hand, our experimental data suggest that the 3D long-range magnetic ordering for Nd ions takes place around $T_{N2} \approx 11$ K. Therefore, we may consider that below T_{c2} (≈ 68 K), and down to $T \approx 20$ K (temperature range where Nd ions are strongly polarized in the internal magnetic field created by the Ni ions), the Nd-Nd interaction is not relevant in comparison with the dominant Nd-Ni one, which bring us to a simple evaluation of the c axis component of the exchange internal field H_i^0 .

Let us first assume that both the Ni^{2+} ferromagnetic component M_{Ni}^0 and H_i^0 are temperature independent in each interval $20 \text{ K} - T_{c3}$ and $T_{c3} - T_{c2}$. We also assume that the high-field magnetic susceptibility is basically related to the contribution of the Nd ions. For instance, in stoichiometric La_2NiO_4 , $\chi_d(T = 4.2 \text{ K}) = 3$ and $\chi_d(T_{c1} = 75 \text{ K}) = 1.4$ (all values are given in 10^{-6} emu/g), while in stoichiometric Nd_2NiO_4 , $\chi_d(T = 4.2 \text{ K}) = 118$ and $\chi_d(T_{c1} = 130 \text{ K}) = 50$. Taking into account all these hypotheses and Eq. (5), Eq. (1) may be written

$$M(H_a, T) = M_{\text{Ni}}^0 + \chi_d(H_i^0 + A\chi_{\text{Ni}}H_a + H_a), \quad (7)$$

where only χ_d has an explicit dependence on temperature and we have ignored the anisotropy field H_k associated with the Nd ions (see Sec. V). Consequently, the zero-field extrapolation of Eq. (7) leads us to a new equation:

$$M_0(T) = M_{\text{Ni}}^0 + \chi_d H_i^0. \quad (8)$$

$M_0(T)$ vs $\chi_d(T)$ is displayed in Fig. 10, which clearly shows four different magnetic behaviors as a function of temperature:

(a) The observed linearity between $M_0(T)$ and $\chi_d(T)$ in the temperature range 20 K– T_{c3} gives full support to our assumption of constant H_i^0 and allows one to derive that $M_{\text{Ni}}^0 = -0.36(7)\mu_B/\text{f.u.}$, i.e., $\theta = 13.1(1)^\circ$, and $H_i^0 = 5.2(6)$ T. M_{Ni}^0 is in close agreement with the value obtained from neutron powder diffraction [$M_{\text{Ni}}^0 = 0.4(2)\mu_B/\text{f.u.}$].⁶ Moreover, it is also evident that in the temperature range T_{c3} – T_{c2} , $M_0(T)$ vs $\chi_d(T)$ also follows a linear law, though the weak ferromagnetic component of the Ni^{2+} magnetic moments M_{Ni}^0 (defined as the crossing point with the y axis) and the internal magnetic field H_i^0 (defined as the slope of the linear law) have been drastically reduced with respect to the former interval 20 K– T_{c3} . Then, we understand that at $T_{c3} \approx 45$ K some kind of sudden spin reorientation of the Ni^{2+} magnetic moments takes place, leading, below this temperature, to a sharp increase in both the weak ferromagnetic component and the canting angle θ , which provokes a marked increase in the internal field acting on Nd ions.

(b) On the other hand, when $T > T_{c2} \approx 68$ K, the extrapolated behavior of $M_0(T)$ vs $\chi_d(T)$ shows that $M_{\text{Ni}}^0 \approx 0$, while the internal magnetic field has been even more drastically reduced, thus signaling that the weak ferromagnetic component of the Ni^{2+} magnetic moments develops below T_{c2} and that some kind of spin reorientation, which should be similar in principle to that observed at T_{c3} , occurs at this temperature.

(c) Finally, below 20 K and down to $T_{N2} \approx 11$ K, M_0 clearly increases. This fact should not be taken as a proof of a consequent increase in the internal field acting on Nd ions due to the Nd-Ni superexchange interaction, but

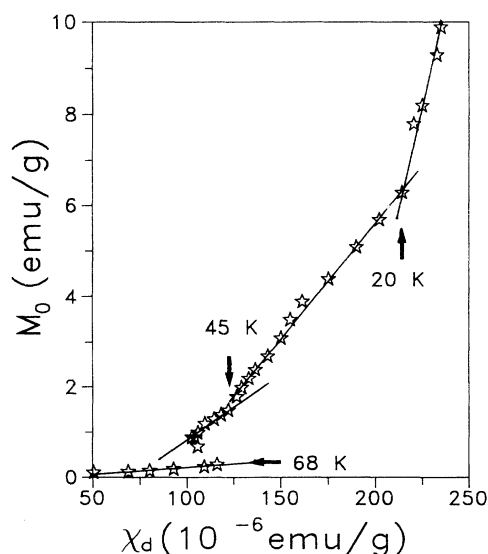


FIG. 10. Saturation magnetization $M_0(T)$ vs high-field differential susceptibility $\chi_d(T)$, showing their linearity in the temperature range 20 K– $T_{c3} \approx 45$ K and T_{c3} – $T_{c2} \approx 68$ K.

rather as the contribution of the magnetocrystalline anisotropy associated with Nd ions, which develops exactly at this temperature (see Sec. V).

We should remark that (i) A NQR investigation on stoichiometric La_2NiO_4 (Ref. 20) demonstrates that the out-of-plane component of the internal field acting on the La sites ($H_i \approx 1.97$ T, which is quite similar to the value we have found in Nd_2NiO_4) is much stronger than that observed in stoichiometric La_2CuO_4 [$H_i \approx 0.1$ T (Ref. 30)], while a simple calculation shows that this relative increase cannot be due to the dipolar interaction thus meaning that the superexchange interaction should be invoked. This is quite understandable if we consider that the Ni-O(2) (apical oxygen) distance is smaller than that of Cu-O(2) [Nd_2NiO_4 : $d(\text{Ni-O}2) = 2.19$ Å; La_2NiO_4 : $d(\text{Ni-O}2) = 2.24$ Å; La_2CuO_4 : $d(\text{Cu-O}) = 2.39$ Å].

(ii) The c component of the internal magnetic field acting on Nd ions at low temperature (20 K– T_{c3}) is much higher than that observed in the T' compounds [Gd_2CuO_4 : $H_i = 0.074$ T (Ref. 27)]. This difference is probably mainly related to the differences in the topology between the K_2NiF_4 and the Nd_2CuO_4 crystal structures. In both the T and T' structures, the TM sublattice is antiferromagnetically aligned and the four nearest-neighbor interactions at the R site cancel by symmetry, in such a way that the net TM- R superexchange coupling arises from next-nearest-neighbor. However, in the T structure there is one additional nearest-neighbor superexchange interaction which is not canceled by symmetry (that connecting the rare-earth and Ni ions through the apical oxygen of the NiO_6 octahedron), while in the T' structure this interaction is absent because of the planar coordination of Cu ions.

(iii) Further, the value of the Ni canting angle θ is not far from that reduced for the Nd and Ni ions from neutron diffraction ($\theta = 18.2^\circ$ and 14.6° , respectively, at 1.5 K).⁶ This slight difference should not be taken as a proof of a noncollinear magnetic structure among Nd and Ni ions. In fact, within the magnetic field range investigated here, M_0 is still increasing, thus indicating that the magnetic domains have not completely disappeared (the domain-wall inversion is not fully accomplished up to $H \approx 8$ T) and so our θ value is only a lower limit.

(iv) Referring to the origin of the spin reorientations at T_{c3} and T_{c2} , we can argue that NPD is unable to distinguish between the two in-plane magnetic modes allowed by the crystallographic symmetry ($g_x + c_y$ and $g_x c_y$) since the low-temperature phase is tetragonal. In this sense, a hypothetical spin reorientation of the Ni^{2+} magnetic moments from the $|110\rangle$ direction to the $|100\rangle$ direction (or *viceversa*) would not be detected. However, this reorientation might have some effects on the ferromagnetic component (f_z) mode, due to the fact that, in both magnetic modes, the relative arrangement of the Ni^{2+} magnetic moments with respect to the tilting axis of the NiO_6 octahedra is different. Although the origin of these spin reorientations is not very clear, it might be related to a change in the local easy magnetization axis associated with the magnetocrystalline anisotropy of Ni ions, leading to the mentioned upturn of the saturation magnetiza-

tion and the high-field magnetic susceptibility (Figs. 8 and 9) at these temperatures. It should be noted that the same kind of in-plane spin reorientations is well-established in Nd_2CuO_4 (Ref. 18) and La_2NiO_4 .¹³

2. Origin of the field-induced transition

The negative sign of M_{Ni}^0 indicates that the Nd-Ni interaction is antiferromagnetic. This result suggests a possible interpretation of the field-induced transition observed in the magnetization curves.

NPD experiments⁶ demonstrate that below $T_{c1} \approx 130$ K a ferromagnetic long-range order of the out-of-plane component of Nd^{3+} magnetic moment appears, standing at an angle of 18.2° with respect to the basal plane at $T = 1.5$ K, thus meaning a value of $1.0(2)\mu_B/\text{Nd}$ atom (the total fitted magnetic moment is $3.2\mu_B/\text{Nd}$ atom), while the out-of-plane component of the Ni^{2+} magnetic moment is about $0.42(2)\mu_B/\text{f.u.}$ which implies that $\theta \approx 14.6^\circ$ (the total fitted magnetic moment is $1.59\mu_B/\text{f.u.}$). On the other hand, since the magnetic domains completely disappear about 8 T, we derive the total saturation magnetization M_0 at $T = 4.2$ K from the magnetization curve $M(H)$ with a maximum applied field of 20 T (Fig. 6) and we obtain that $M_0 = 2.25\mu_B/\text{f.u.}$

On the basis of this framework, the origin of the field-induced transition may be viewed as follows: when the applied field equals the critical field $H_{\text{cr}} = 5.2(2)$ T, the ferromagnetic component of Ni^{2+} ions, which lay antiparallel to that of Nd^{3+} ions, undergoes a metamagnetic-like transition, and both out-of-plane components become parallel (Fig. 11). Then, we observe a jump in the $M(H)$ curve, which is not abrupt but smooth, due to the fact that our sample is polycrystalline. Then, when $H_a > H_{\text{cr}}$ we may write the total saturation magnetization as

$$M_0 = 2M_{\text{Nd}}^0 + M_{\text{Ni}}^0. \quad (9)$$

From our data [$M_0 = 2.25\mu_B/\text{f.u.}$ at $T = 4.2$ K and $M_{\text{Ni}}^0 = 0.36(7)\mu_B/\text{f.u.}$, independent of temperature], we find that $M_{\text{Nd}}^0 = 0.95(14)\mu_B/\text{Nd}$ at $T = 4.2$ K, which is comparable with that derived from NPD at $T = 1.5$ K ($M_{\text{Nd}}^0 = 1.0(2)\mu_B/\text{Nd}$).

The fact that both the critical field (at which the metamagnetic transition takes place) and the internal magnetic field (that reflects the net superexchange coupling Nd-Ni) are equal within the experimental error, gives full support to our assumption of the origin of the field-induced transition. Let us consider an uniaxial antiferromagnet where the applied field is parallel to the easy magnetization axis. When the anisotropy is high, which is in fact the case since the coercive field is enormous and the domain wall inversion is not fully accomplished till 8 T, the antiferromagnetic ordering is stable up to $H_a < H_i^0$, in such a way that when $H_a > H_i^0$ the magnetic moments become ferromagnetically ordered.³ Then, the out-of-plane components of both Ni and Nd ions lie antiparallel exactly until the applied field equal the internal field.

C. $T < T_{N2}$

It seems experimentally well established that the Nd^{3+} ions become antiferromagnetically ordered at $T_{N2} = 11$ K,

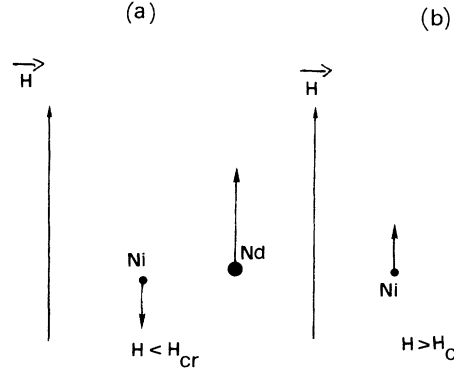


FIG. 11. Scheme of the relative arrangement among the weak ferromagnetic components of Nd^{3+} and Ni^{2+} sublattices when (a) the applied magnetic field H is smaller than the critical field H_{cr} and (b) the applied magnetic field H is larger than the critical field H_{cr} .

although no specific-heat results have been reported up to now. On lowering temperature below T_{N2} , no abrupt change is observed in $M_0(T)$, though this magnitude smoothly tends to the saturation regime [Fig. 9(b)]. Then, if the out-of-plane component of the Ni^{2+} magnetic moments M_{Ni}^0 does not significantly vary from that value we have obtained in the paramagnetic phase of the R ($T > T_{N2}$), $M_0(T)$ is basically governed by the behavior of the out-of-plane component of the Nd^{3+} ions. Then, the c axis component of the internal field acting on these ions is not modified by their long-range ordering of Nd ions and M_0 smoothly increases since Nd ions are not yet saturated. This leads to the conclusion that both the $J_{\text{Nd-Ni}}$ and $J_{\text{Nd-Nd}}$ superexchange interactions do not compete with each other, which is consistent with the reported magnetic structure if the $J_{\text{Nd-Nd}}$ interaction is antiferromagnetic.

Finally, the high-field magnetic susceptibility χ_d [Fig. 8(a)] displays a sharp peak at T_{N2} , reflecting an antiferromagnetic ordering of the in-plane component of Nd ions, and tends to zero when $T \rightarrow 0$. This might be due to the crystal-field energy-level splitting of Nd ions at low temperature arising from the crystallographic symmetry.

V. MAGNETIC INTERACTIONS

Let us assume that the magnetic Hamiltonian describing the magnetic interactions in Nd_2NiO_4 may be written as follows:

$$\begin{aligned} \mathbb{H} = & J_{\text{Ni-Ni}} \sum_{\text{NN}} \mathbf{S}_i^{\text{Ni}} \cdot \mathbf{S}_j^{\text{Ni}} \\ & + J'_{\text{Ni-Ni}} \sum_{\text{NNN}} \mathbf{S}_i^{\text{Ni}} \cdot \mathbf{S}_j^{\text{Ni}} + \mathbf{D}_{\text{Ni-Ni}} \sum_{\text{NN}} \mathbf{S}_i^{\text{Ni}} \times \mathbf{S}_j^{\text{Ni}} \\ & + J_{\text{Nd-Ni}} \sum_{\text{NN}} \mathbf{S}_i^{\text{Nd}} \cdot \mathbf{S}_j^{\text{Ni}} + K^{\text{Nd}} \sum_i (\mathbf{n} \cdot \mathbf{s}_i)^2, \end{aligned} \quad (10)$$

where all the sums are extended to nearest neighbors, except for the second one which is extended to next-nearest neighbors, and the last one which is extended to all the

Nd ions in the sample. $J_{\text{Ni-Ni}}$ and $\mathbf{D}_{\text{Ni-Ni}}=(0, D_{\text{Ni-Ni}}, 0)$ stand respectively for the in-plane symmetric and antisymmetric parts of the antiferromagnetic Ni-Ni superexchange interaction, while $J'_{\text{Ni-Ni}}$ stands for the magnetic interactions between two adjacent NiO₂ planes. $J_{\text{Nd-Ni}}$ is the isotropic symmetric antiferromagnetic Nd-Ni superexchange coupling constant. Moreover, in Eq. (10) we have assumed the magnetocrystalline anisotropy of Nd ions to be uniaxial, thus meaning that \mathbf{n} and \mathbf{s} stand for, respectively, the unitary vectors along the c axis and along the direction defined by the Nd magnetic moments. Then, K^{Nd} represents the anisotropy energy per Nd spin, and is related to the first anisotropy constant K_1^{Nd} through

$$K_1^{\text{Nd}} = K^{\text{Nd}}(z'/V_{\text{uc}}), \quad (11)$$

where z' is the number of Nd ions per unit cell and V_{uc} is the volume of the unit cell. In Eq. (10), we have ignored for simplicity the antisymmetric Ni-Nd superexchange interaction $D_{\text{Nd-Ni}}$ and the symmetric Nd-Nd $J_{\text{Nd-Nd}}$. In this sense, it is obvious that our magnetic Hamiltonian is not able to take into account the long-range magnetic ordering of Nd³⁺ ions.

Labeling θ and θ' as the canting angles, respectively, of the Ni and Nd magnetic moments with the a - b plane and minimizing the system energy with respect to θ and θ' , the equilibrium state will be reached when

$$\begin{aligned} -4J_{\text{Ni-Ni}}S^{\text{Ni}}S^{\text{Ni}}\sin(2\theta) - 8J'_{\text{Ni-Ni}}S^{\text{Ni}}S^{\text{Ni}}\sin(2\theta) \\ + 4 \cdot D_{\text{Ni-Ni}}S^{\text{Ni}}S^{\text{Ni}}\cos(2\theta) \\ - 10J_{\text{Nd-Ni}}S^{\text{Ni}}S^{\text{Nd}}\sin(\theta + \theta') = 0, \quad (12) \end{aligned}$$

$$-5J_{\text{Nd-Ni}}S^{\text{Ni}}S^{\text{Nd}}\sin(\theta + \theta') - 4K^{\text{Nd}}\sin\theta'\cos\theta' = 0, \quad (13)$$

and knowledge of the magnetic interactions ($J_{\text{Ni-Ni}}$, $D_{\text{Ni-Ni}}$, $J'_{\text{Ni-Ni}}$, $J_{\text{Nd-Ni}}$, K^{Nd}) will lead us to the determination of the magnetic structure, which is parametrized by (θ', θ) .

A. Magnetic interactions at 0 K

Concerning $J_{\text{Ni-Ni}}$, Aeppli *et al.*⁴ found that $J_{\text{Ni-Ni}} \approx -20$ meV in La₂NiO₄. When moving from La₂NiO₄ to Nd₂NiO₄, the superexchange angle φ decreases, due to the fact that the tilting angle of the NiO₆ octahedra increases, and the in-plane superexchange distance $d = \text{O}(1)\text{-Ni-O}(1)$ increases^{6,11} in such a way that both effects tend to reduce the in-plane magnetic interaction. Assuming the well-known dependences of the superexchange coupling constant J with respect to φ (Ref. 32) and d ,³³

$$J(\varphi) = J_0 \cos^2 \varphi, \quad J(d) = J'_0 d^{-12} \quad (14)$$

and taking into account those values of the superexchange angles and distances determined by NPD,^{6,11} we expect to obtain a relative decrease of about 5% in the in-plane antiferromagnetic exchange interaction $J_{\text{Ni-Ni}}$ when moving from La₂NiO₄ to Nd₂NiO₄, thus meaning that $J_{\text{Ni-Ni}}(\text{Nd}_2\text{NiO}_4) \approx -19$ meV.

On the other hand, let us assume that the strong bidi-

imensionality of the crystallographic structure makes Nd₂NiO₄ a good example of the two-dimensional antiferromagnetic Heisenberg model.^{34,35} We may also assume that the 3D long-range antiferromagnetic ordering appears because of the intraplane interaction $J'_{\text{Ni-Ni}}$. It is worth noting that $J'_{\text{Ni-Ni}}$ is a super-superexchange coupling that cancels by symmetry at nearest neighbors when the structure is tetragonal type K₂NiF₄. In this basic framework, the two-dimensional in-plane antiferromagnetic correlation length l increases upon lowering temperature, and when the effective interplane interaction $[l(T)/a]^2 J'_{\text{Ni-Ni}}$ (a stands for the in-plane cell parameter) becomes comparable to the thermal energy $K_B T$, a 3D ordering occurs. Then, at the Néel temperature, we can write^{4,18}

$$(M_s/M_0)^2 [l(T_N)/a]^2 J' \approx K_B T_N, \quad (15)$$

where the factor M_s/M_0 accounts for the relative importance of the zero-point quantum fluctuations,³⁶ which are enhanced in the 2D Heisenberg antiferromagnetic systems. In Nd₂NiO₄, the $S=1$ spin reduction is about 20% ($M_s \approx 1.59\mu_B$,⁶ $M_0 \approx 2\mu_B$). Equation (15) shows that knowledge of the in-plane correlation length at the Néel temperature $l(T_N)$ is necessary in order to determine the interplane interaction $J'_{\text{Ni-Ni}}$. Chakravarty, Halperin, and Nelson³⁴ have recently developed a quantitative theory (CHN theory) to account for the temperature-dependence of the instantaneous spin-spin antiferromagnetic in-plane correlation length in the 2D Heisenberg models, which may be written as follows

$$S=1: \quad l/a = C \exp[2\pi\rho_s/K_B T] / (1 + K_B T/2\pi\rho_s), \quad (16)$$

where $C \approx 0.17$ and ρ_s is the spin stiffness constant.^{34,35} From our data ($J_{\text{Ni-Ni}} \approx -19$ meV and $T_N = 320$ K, Eq. (16) leads to $l(T_N)/a \approx 4.5$. Then, we derive $J'_{\text{Ni-Ni}} \approx -2.2$ meV from Eq. (15). It is remarkable that, as compared to La₂NiO₄, the effective in-plane correlation length has been reduced by a factor 0.75, while the interplane interaction has been multiplied by a factor of 2 [La₂NiO₄: $l(T_N)/a \approx 6.1$; $J'_{\text{Ni-Ni}} \approx -1.1$ meV (Ref. 13)]. We believe that the former is caused by the relative reduction in the intraplane superexchange interaction $J_{\text{Ni-Ni}}$ (La₂NiO₄: $J_{\text{Ni-Ni}} \approx -20$ meV; Nd₂NiO₄: $J_{\text{Ni-Ni}} \approx -19$ meV), while the latter is due to the relative decrease of the apical distance Ni-O(2) of the NiO₂ octahedra, through which the interplane superexchange interaction proceeds [La₂NiO₄: $d(\text{Ni-O}(2)) = 2.24$ Å;¹¹ Nd₂NiO₄: $d(\text{Ni-O}(2)) = 2.19$ Å (Ref. 6)].

Finally, Eq. (8) has led us to determine the weak ferromagnetic component of the Ni magnetic moment [$M_{\text{Ni}}^0 = -0.36(7)\mu_B/\text{f.u.}$, i.e., $\theta = 13.1(1)^\circ$] and the c -axis component of the internal magnetic field acting on Nd ions [$H_i^0 = 5.2(6)$ T]. We should remark that both values are constant in the temperature range 20 K– T_{c3} and in this evaluation we have neglected the anisotropy field acting on Nd ions. In this framework and on the scope of the mean-field approximation, the fitted H_i^0 and M_{Ni}^0 led us to a first evaluation of an isotropic exchange coupling

$J_{\text{Nd-Ni}}$ by using the formula

$$H_i^0 = 2ZJ_{\text{Nd-Ni}}M_{\text{Ni}}^0 / Ng_{\text{Ni}}g_{\text{Nd}}\mu_B^2 \quad (17)$$

from which we obtain that $J_{\text{Nd-Ni}} = -0.6(2)$ meV. We have not found any thorough evaluation of the R -TM superexchange coupling in these kinds of oxides. For example, Dalichaouch *et al.*³⁷ report that an abrupt upturn on the upper critical field of superconducting $\text{Sm}_{1.85}\text{Ce}_{0.15}\text{CuO}_{4-y}$, as compared to superconducting $\text{Nd}_{1.84}\text{Ce}_{0.16}\text{CuO}_{4-y}$, takes place as soon as the Sm sublattice orders antiferromagnetically along the c axis at $T_{N2} \approx 4.9$ K, and from the temperature dependence of the upper critical field they derive that the exchange interaction between the localized Sm magnetic moments, and the spin of the superconducting charge carriers is about $J \approx 60$ meV. However, the two values (Nd_2NiO_4 : $J_{\text{Nd-Ni}} \approx -0.6$ meV; $\text{Sm}_{1.85}\text{Ce}_{0.15}\text{CuO}_{4-y}$: $J \approx 60$ meV) are not directly comparable, since in our case we are dealing with an interaction among localized spins, while in superconducting Sm-Ce conduction electrons are delocalized.

As we can see, at 0 K our set of five parameters ($J_{\text{Ni-Ni}} \approx -19$ meV, $J'_{\text{Ni-Ni}} \approx -2.2$ meV, $J_{\text{Nd-Ni}} \approx -0.6$ meV, $\theta \approx 13.1^\circ$, and $\theta' \approx 18.2^\circ$), besides Eqs. (11), (12), and (13), allows us to obtain

$$\begin{aligned} D_{\text{Ni-Ni}} &\approx -16 \text{ meV}, \\ K^{\text{Nd}} &\approx 4.6 \text{ meV}; \quad K_1^{\text{Nd}} \approx 1.7 \times 10^8 \text{ erg/cm}^3. \end{aligned} \quad (18)$$

Concerning the first anisotropy constant associated with Nd ions, K_1^{Nd} is roughly the order of magnitude of the typical values of rare earths ($K_1^{\text{Nd}} = 1.6 \times 10^8$ erg/cm³ in a $\text{Nd}_2\text{Fe}_{14}\text{B}$ single crystal,³⁸ thus meaning that the anisotropy of Nd_2NiO_4 is very large at low temperature.

Referring to the antisymmetric Ni-Ni superexchange interaction $D_{\text{Ni-Ni}}$, the huge relative increase with respect to La_2NiO_4 (La_2NiO_4 : $D_{\text{Ni-Ni}} \approx -0.1$ meV;¹³ Nd_2NiO_4 : $D_{\text{Ni-Ni}} \approx -16$ meV) is on the origin of the consequent increase of the canting angle θ of the Ni^{2+} magnetic moments with respect to the basal plane (θ varies from 0.14° to 13.1° on moving from La_2NiO_4 to Nd_2NiO_4). On the other hand, the antisymmetric should be proportional to the overlap between the $d_{x^2-y^2}$ orbitals of neighboring sites, which, at the same time, increases with the tilting angle of the NiO_6 octahedra. This tilting angle is greater in Nd_2NiO_4 (Ref. 6) than in La_2NiO_4 .¹¹

B. Canting angles θ and θ' as a function of temperature

In Eqs. (12) and (13), only K^{Nd} has an explicit dependence on temperature. Let us assume that the temperature dependence of first anisotropy constant for rare-earth elements may be written³¹

$$K_1^{\text{Nd}}(T) = K_1^{\text{Nd}}(T=0)[M(T)/M(0)]^3, \quad (19)$$

where $M(T)$ is spontaneous magnetization at a given temperature and M_0 is the spontaneous magnetization at zero kelvin. NPD diffraction shows³⁹ (i) the a - b component of the Nd ions magnetic moments is about $0.1\mu_B/\text{Nd}$ atom at 68 K, and increases to $0.5\mu_B$ at 45 K

and to $1\mu_B/\text{Nd}$ atom at 20 K, and (ii) the c component is below the detection level about 20 K, and it is about $0.05\mu_B/\text{Nd}$ atom at this temperature. From these data, Eq. (19) determines that, at 20 K, $K_1^{\text{Nd}} = 5.1 \times 10^6$ erg/cm³ and $K^{\text{Nd}} = 0.13$ meV, which is about the 3% of the value at 0 K, while at 45 K $K_1^{\text{Nd}} = 6.8 \times 10^5$ erg/cm³ and $K^{\text{Nd}} = 0.017$ meV, which is about the 0.4% of the value at 0 K. Then, we understand that the Nd-ion anisotropy will be high at low temperature (the large increase of the coercive field at low temperature—see Fig. 5—reinforces this assertion) and it is in no way relevant above 20 K, thus meaning that in the determination of H_i^0 [Eqs. (6)–(8)] it is not worth taking into account. Finally, NPD shows that the Nd-ion canting angle θ' is practically zero above 20 K, from which we believe that the origin of both the huge increase in the ferromagnetic component at low temperature shown by NPD and also the upturn of $M_0(T)$ (Fig. 10) below 20 K should be related to the magnetic anisotropy associated with Nd ions.

On the other hand, as soon as we know the temperature dependence of K^{Nd} , Eqs. (12) and (13) will allow us to ascertain the temperature dependence of the canting angle θ and θ' . At 45 K, we derive that $\theta = 13.4^\circ$ and $\theta' = 0^\circ$, while at 20 K the best solution to our equation system is obtained when $\theta = 13.5^\circ$ and $\theta' \rightarrow 0^\circ$. It is now clear that the canting angle θ of the magnetic moments of Ni ions, and consequently the weak ferromagnetic component M_{Ni}^0 , does not change in the temperature range $20 \text{ K} - T_{c3}$, giving further support to the way we have derived $J_{\text{Nd-Ni}}$. It is also obvious that from our proposed magnetic Hamiltonian [Eqs. (12) and (13)] we are not able to account for any discontinuous phenomena. In this sense, the spin reorientation observed at T_{c3} is beyond our goals and cannot be explained in this framework, which is nevertheless valid, in principle, when $T < T_{c3}$.

VI. SUMMARY AND CONCLUSIONS

We have analyzed the complex magnetic behavior observed in stoichiometric antiferromagnetic Nd_2NiO_4 oxide. It is found that the interactions associated with the Nd^{3+} ions lead to a temperature-dependent weak ferromagnetic behavior, to a magnetic structure where the Nd and Ni magnetic moments are not collinear, and finally to a magnetic-field-induced (metamagneticlike) transition. It is also stressed that the Nd magnetic moments present a long-range magnetic ordering at low temperature, which is probably mediated by the polarization effect associated with the internal field created by the Ni magnetic moments.

The leading microscopic magnetic interactions have been discussed taking into account the analysis carried out for stoichiometric La_2NiO_4 . The magnetic properties of the latter have been recently shown¹³ to be easily investigated in the scope of the 2D Heisenberg model proposed by Chakravarty *et al.*³⁴ We have assumed that the essential features of this model are also valid for Nd_2NiO_4 and hence we obtain a set of symmetric and antisymmetric superexchange interactions associated with Ni ions. Furthermore, the Ni-Nd exchange is also determined and it is evidenced in some experimental features,

i.e., the paramagnetic behavior in the collinear high-temperature antiferromagnetic phase, the field-induced transition, the strongly enhanced weak ferromagnetic component, etc.

Finally, several experimental results have forced us to introduce a uniaxial single-ion contribution of Nd ions to the magnetic anisotropy in the magnetic Hamiltonian describing the magnetic interactions of this oxide. We have shown that both this term and the strong enhancement of the antisymmetric $D_{\text{Ni-Ni}}$ interaction, as compared to La_2NiO_4 , allow us to explain the appearance of very large canting angles for the Ni and Nd magnetic moments.

As a final conclusion, our study shows that even if the magnetic behavior of both Nd_2CuO_4 and Nd_2NiO_4 is highly complex, some severe differences in the rare-earth transition-metal interaction exist. The T' cuprates seem to have, in some cases, a weak ferromagnetic component which appears within the a - b plane, while the ferromagnetic component in Nd_2NiO_4 is along the c axis. The origin of these ferromagnetic components in the T' structure and how they interact with the rare-earth ions is still

an object of discussion. From our study, it may be inferred which are those magnetic interactions that should be also taken into account in the T' structure. This is a problem that now holds a strong interest in the context of understanding the relationship between high-temperature superconductivity and magnetism.³⁷⁻⁴⁰

ACKNOWLEDGMENTS

We are indebted to M. Vallet, J. González-Calbet and J. Alonso, for making available to us the sample used in this work. We would like to thank J. Rodríguez-Carvajal and J. L. Martínez for communicating neutron diffraction results prior to publication, and M. Tovar, for all his suggestions and discussions regarding the magnetic properties of Nd_2NiO_4 . We are also grateful to J. Tejada, and M. Pernet, for their experimental assistance in the SQUID and High-Field measurements, respectively. This work has been funded by the Spanish CICYT Project No. MAT88-0163-C03-C02, the Spanish DGICYT Project No. PB89-71, the EEC Project NSCI-0036-F, and the Spanish MIDAS program.

*Author to whom all correspondence should be addressed.

¹J. G. Bednorz and K. A. Müller, *Z. Phys. B* **64**, 189 (1986); Y. Tokura, H. Tahaki, and S. Uchida, *Natura* **337**, 335 (1989).

²Z. Kakol, J. Spalek, and J. M. Honig, *J. Solid State Chem.* **79**, 288 (1989).

³R. J. Birgeneau and G. Shirane, in *Physical Properties of High Temperature Superconductors*, edited by D. M. Ginsberg (World Scientific, Singapore, 1989), and references therein; see also, Y. Endoh *et al.*, *Phys. Rev. B* **37**, 7443 (1988).

⁴G. Aeppli and D. J. Buttrey, *Phys. Rev. Lett.* **61**, 203 (1988).

⁵S. Ghamaty, B. W. Lee, J. T. Market, E. A. Early, T. Bjornholm, C. L. Seaman, and M. B. Maple, *Physica C* **160**, 217 (1989); M. F. Hudley, J. D. Thompson, S.-W. Cheong, Z. Fisk, and S. B. Oseroff, *ibid.* **158**, 102 (1989).

⁶J. Rodríguez-Carvajal, M. T. Fernández, J. L. Martínez, F. Fernández, and R. Saez-Puche, *Europhys. Lett.* **11**, 261 (1990).

⁷X. Obradors, X. Batlle, J. Rodríguez-Carvajal, J. L. Martínez, M. Vallet, J. González-Calbet, and J. Alonso, *Phys. Rev. B* **43**, 10451 (1991).

⁸M. T. Fernández-Díaz, J. Rodríguez-Carvajal, J. L. Martínez, G. Fillion, F. Fernández, and R. Saez-Puche, *Z. Phys. B* **82**, 275 (1991).

⁹X. Batlle, B. Martínez, X. Obradors, J. Rodríguez-Carvajal, J. L. Martínez, and P. Odier, *J. Appl. Phys.* (to be published).

¹⁰J. Rodríguez-Carvajal, J. L. Martínez, J. Pannetier, and R. Saez-Puche, *Phys. Rev. B* **38**, 7148 (1988).

¹¹J. Rodríguez-Carvajal, M. T. Fernández, and J. L. Martínez, *J. Phys. Condensed Matter* **3**, 3215 (1991).

¹²S. W. Cheong, J. D. Thompson, and S. Fisk, *Physica C* **158**, 109 (1989).

¹³X. Batlle, X. Obradors, M. Vallet, J. González-Calbet, and M. J. Sayagués (unpublished).

¹⁴G. H. Lander, P. J. Brown, J. M. Honig, and Z. Spalek, *Phys. Rev. B* **40**, 4463 (1989).

¹⁵J. D. Axe, H. Moudden, D. Holhwein, D. E. Cox, K. M. Mohanty, A. R. Moodenbaugh, and Y. Xu, *Phys. Rev. Lett.*

62, 2571 (1989).

¹⁶D. C. Johnston, J. P. Stokes, D. P. Gosborn, and J. T. Lewandowski, *Phys. Rev. B* **36**, 4007 (1987).

¹⁷C. L. Seaman, N. Y. Ayoub, T. Bjornholm, E. A. Early, S. Ghamaty, B. W. Lee, J. T. Market, J. J. Neumeier, P. K. Tsai, and M. B. Maple, *Physica C* **159**, 391 (1989).

¹⁸S. Skanthakumar, H. Zhang, T. W. Clinton, W. H. Li, J. W. Lynn, Z. Fisk, and S. W. Cheong, *Physica C* **160**, 124 (1989); see also M. Matsuda *et al.*, *Phys. Rev. B* **42**, 10098 (1990).

¹⁹S. W. Cheong, J. D. Thompson, and S. Fisk, *Phys. Rev. B* **39**, 4395 (1989).

²⁰T. Thio, T. R. Thurston, N. W. Preyer, P. J. Picone, M. A. Kastner, H. P. Jenssen, D. R. Gabbe, C. Y. Chen, R. J. Birgeneau, and A. Aharony, *Phys. Rev. B* **38**, 905 (1988).

²¹R. Sáez-Puche, J. L. Rodríguez, and F. Fernández, *Inorg. Chem. Acta* **140**, 151 (1987).

²²R. Sáez-Puche, M. Norton, T. R. White, and W. S. Glausinger, *J. Solid State Chem.* **50**, 281 (1983).

²³S. B. Oseroff, D. Rao, F. Wright, D. C. Vier, S. Shultz, J. D. Thompson, Z. Fisk, S. W. Cheong, M. F. Hundley, and M. Tovar, *Phys. Rev. B* **41**, 1934 (1990).

²⁴R. L. Carlin and A. J. van Duyneveldt, in *Magnetic Properties of Transition Metal Compounds* (Springer-Verlag, New York, 1977).

²⁵H. A. Groenendijk, A. J. van Duyneveldt, and R. D. Willet, *Physica B* **101**, 320 (1980).

²⁶A. J. van Duyneveldt, *J. Appl. Phys.* **53**, 8006 (1982).

²⁷J. D. Thompson, S. W. Cheong, S. E. Brown, S. Fisk, S. B. Oseroff, M. Tovar, D. C. Vier, and S. Shultz, *Phys. Rev. B* **39**, 6660 (1989).

²⁸X. Batlle, B. Martínez, X. Obradors, and M. Tovar (unpublished).

²⁹S. Wada, T. Kobayashi, M. Kabugari, K. Shibutani, and R. Ogawa (private communication).

³⁰Y. Kitaoka, S. Hiramatsu, T. Tokara, K. Asayama, K. Ohishi, M. Kikuchi, and N. Kobayashi, *Jpn. J. Appl. Phys.* **26**, 397 (1987).

- ³¹A. Herpin, *Theorie du Magnétisme* (P.U.F., Paris, 1968).
- ³²G. A. Sawatzky and F. van der Woude, *J. Phys. (Paris) Colloq.* **12**, C6-47 (1972); B. C. Tofield, *ibid.* **37**, C6-539 (1976).
- ³³L. J. De Jongh and R. Block, *Physica B+C* **79B**, 568 (1975).
- ³⁴S. Chakravarty, B. I. Halperin, and D. R. Nelson, *Phys. Rev. Lett.* **60**, 1057 (1988); *Phys. Rev. B* **39**, 2344 (1989).
- ³⁵R. J. Birgeneau, *Phys. Rev. B* **41**, 2514 (1990); see also L. J. de Jongh and A. R. Miedema, *Adv. Phys.* **23**, 1 (1975); R. J. Birgeneau, J. Skalko, and G. Shirane, *Phys. Rev. B* **3**, 1736 (1971).
- ³⁶P. W. Anderson, *Phys. Rev.* **86**, 694 (1952).
- ³⁷Y. Dalichaouch, B. W. Lee, C. L. Seaman, J. T. Market, and M. P. Maple, *Phys. Rev. Lett.* **64**, 599 (1990).
- ³⁸*Handbook on the Physics and Chemistry of Rare Earths*, edited by K. A. Gschneider, Jr., and L. Eyring (North Holland/Elsevier, Amsterdam, 1989), Vol. 12.
- ³⁹J. Rodríguez-Carvajal (private communication).
- ⁴⁰J. J. Neumeier, T. Bjornholm, M. B. Maple, and I. K. Schuller, *Phys. Rev. Lett.* **63**, 2516 (1989).